Biomass Conversion and Biorefinery (2023) 13:7677–7685
https://doi.org/10.1007/s13399-021-01664-x

ORIGINAL ARTICLE

Investigating the bioenergy potential of invasive Reed Canary (*Phalaris arundinacea*) through thermal and kinetic analyses

Hesham Alhumade[1,2] · Muhammad Sajjad Ahmad[3,4] · Emanuele Mauri[5] · Yusuf Al-Turki[6] · Ali Elkamel[4]

Received: 24 April 2021 / Revised: 11 June 2021 / Accepted: 16 June 2021 / Published online: 1 July 2021

Abstract

The thermal conversion of biomass plays an important role in the development of energy reaping technologies and fire engineering. The study investigates the bioenergy potential of Reed Canary (*Phalaris arundinacea*) through investigating the combustion kinetics and thermal behavior. Reed Canary samples were collected from various rural areas of Ontario, Canada. Four heating rates (10, 20, 30, and 40 °C min^{-1}) were utilized to perform the thermal degradation analysis using a thermogravimetric analyzer. Three different stages were identified ranging from 25 °C to 800 °C in which major degradation stage had two regions from 210 °C to 530 °C where most of the biomass changed into products. Furthermore, isoconversional models including Kissenger-Akahira-Sunose (KSA), Starink and Flynn–Wall–Ozawa (FWO) were used to evaluate the reaction kinetics such as the activation energy and the pre-exponential factor. The reported kinetics parameters demonstrate the promising potential of Reed Canary for bioenergy production. Moreover, the low cost and the abundance of Reed Canary facilitate the possibility of introducing the biomass as a cost efficient and environmentally friendly natural resource for renewable bioenergy production.

Keywords Invasive Reed Canary · Combustion · Thermal behavior · Bioenergy

1 Introduction

The global energy demand is increasing rapidly due to the fast growth in population and modern development of various industrial sectors [1]. For decades, fossil fuel has been utilized as the primary source of energy despite the associated major environmental impact [2]. Indeed, the combustion of fossil fuel contributes to the emission of a significant amount of greenhouse gases such as CO_2 and CH_4. Moreover, the growing consumption of fossil fuel will definitely lead to depletion of such a natural resource in the future [3]. Therefore, an increasing number of studies have been devoted to explore alternative sustainable and renewable resources of energy [4]. Examples of renewable resources of energy include wind power, solar energy, geothermal energy, and the conversion of the biomass and industrial wastes to bioenergy. There are different geographical factors that limit the utilization of wind, geothermal and solar as sustainable resources of clean energy, whereas, there are various types of biomass and industrial waste resources globally [5]. For example, the vision of the relevant policies facilitates the growth of bioenergy consumption in Europe to reach 61.2% of the annually total renewable energy consumption [6]. Therefore, a number of technologies are currently developed to explore the potential of biomass waste for bioenergy production. Among the promising technologies in biomass waste conversion to fuel are pyrolysis, combustion and gasification [5]. The low emission of air pollutants and the

✉ Ali Elkamel
aelkamel@uwaterloo.ca

1 Department of Chemical and Materials Engineering, Faculty of Engineering, King Abdulaziz University, Jeddah 21589, Saudi Arabia

2 Center of Research Excellence in Renewable Energy and Power Systems, King Abdulaziz University, Jeddah 21589, Saudi Arabia

3 Department of Chemical Engineering, Hebei University of Technology, Tianjin, China

4 Department of Chemical Engineering, University of Waterloo, Waterloo, Canada

5 Department of Engineering, Università Campus Bio-Medico Di Roma, via Álvaro del Portillo 21, 00128 Rome, Italy

6 Department of Electrical and Computer Engineering, Faculty of Engineering, King Abdulaziz University, Jeddah 21589, Saudi Arabia

carbon neutral characteristics of biomass drive the potential of biomass consumption as renewable resource of energy.

Plant biomass is a typical source of biomass waste that can be utilized for renewable energy purposes using various approaches [7]. For instance, thermogravimetric analysis (TGA) is considered as one of the cost efficient, simple, and very effective technique to explore the thermal decomposition behavior of biomass during a combustion process [8]. Carbon dioxide will be released during combustion and can be consumed by plant. In addition, the conversion of plant biomass will deliver minimal amount of ash, sulphur and nitrogen, which supports the environmental friendly characteristic of plant biomass as promising source of renewable energy [9]. Although the combustion behavior of biomass depends mainly on the chemical composition of the biomass, factors of the combustion process will influence the conversion process. These factors include the heating rate, conversion environment, residence time and pressure [10]. Therefore, it is important to explore the combustion condition to understand the combustion behavior of a plant biomass before considering the biomass for bioenergy application [11]. For this purpose, researchers have developed different kinetic models to evaluate significant kinetic parameters such as activation energy (E_a), pre-exponential factor (A), and reaction order (n). Various plant biomasses were investigated for bioenergy application including but not limited to *Sida cordifolia* L. [12], *Pear millet* [13], *Pine wood* [14] and *pistachio shell* [15]. Although various feedstock and biomass waste were evaluated as potential resources for sustainable and renewable bioenergy, there are some challenges that may seize the opportunity for utilizing these resources for bioenergy production. Direct competition with food crops, chemical composition, and the impact in ecological diversity are examples of those challenges [13]. Therefore, researchers are continuously searching for plant biomass that can be utilized for bioenergy application with optimal chemical composition reflected by the minimum lignin content and least negative impact on the environment.

An example of the plant biomass that can be explored for bioenergy application is Reed Canary grass (RC), which is one of the Eurasian cultivars that were in brought to North America as a marginal land product and livestock need. However, it was noticed that the invasive characteristic of RC might threat the biodiversity and the modern development of society in several ways. For instance, the fast growth of RC in wetlands represents a threat for the availability and biodiversity of wetland various species. In addition, the invasive characteristic of RC allows the plant biomass to grow rapidly and cause clogging of waterways, which increases the risk of flooding. The fast growing of RC triggers the need for a solution that attenuate the population of RC species in wetland with minimum impact on the environment. Inspired by the need to attenuate the spreading of RC, propose an environmental friendly approach and the growing need to explore various resources for sustainable and renewable energy purpose, this study was conducted to evaluate RC as a potential resource for bioenergy production. The combustion behavior of RC was examined using TGA at various heating rates to demonstrate the combustion characteristic of the biomass. In addition, the composition of the plant biomass was studied using elemental analysis.

2 Materials and methods

2.1 Sample preparation and characterization

Reed Canary samples were collected from various rural areas of Ontario, Canada and the biomass is widely spread in North America. Preparing the RC samples for analysis starts with cleaning the samples with double distilled water and allowing the samples to dry under natural sunlight for few days. The moisture residue for the washing process was further removed in an oven at 100 °C for 2 h. Then the samples were grinded with a micro-mill grinder to obtain average particle size of 150–200 µm to avoid heat and mass transfer limitations during the proximate and thermogravimetric analysis. Proximate analysis was conducted to determine the solid, moisture, and volatile matter contents of RC, where the analysis was carried out following the protocol described in standards ASTM-E781 and ASTM-E1755. First, 10 mg of cleaned biomass samples were dried in a vacuum oven at 105 °C for two days and the observed mass loss was reported as the moisture content of the samples (MC%). The dried samples were then placed in a crucible at 970 °C in inert environment in a muffle furnace and the observed loss in mass was reported as the volatile matter (VM%). The ash content was computed by oxidizing the cleaned and dried biomass sample at 815 °C, where the residue was reported as the ash content. Finally, the fixed carbon content (FC%) was computed using the following equation:

$$FC(\%) = 100 - \ (ash\ \ content + VM + moisture) \tag{1}$$

In addition, all proximate analyses were carried out in triplicate to examine the repeatability of the reported results.

Elemental analyzer was utilized to conduct the ultimate analysis of the biomass sample. Here, the cleaned and dried biomass samples were examined to determine the carbon, sulphur, nitrogen and hydrogen contents, while the residue was reported as oxygen content.

2.2 TGA experiments

The TGA were performed in triplicates to insure the accuracy of results at four different heating rates (10, 20, 30, and

40 °C min^{-1}) with particle size ranging from 150 to 300 µm in STA-409 (NETZSCH-Gerätebau). The 10 mg mass was used to conduct experiments with 100 mL continuous air flow in the reaction chamber. Sample was heated from normal room temperature to 800 °C in the aluminum crucibles. The temperature was elevated continuously at each heating rate with uniform mass degradation pattern.

2.3 Mathematical model development

Thermogravimetric conversion rate can be calculated as;

$$\alpha = \left(m_i - m_t\right) / \left(m_i - m_f\right) \tag{2}$$

where m_i, m_t, and m_f refer to initial, change in mass at time t and final masses, respectively.

The decomposition rate of the sample can be written as;

$$\frac{d\alpha}{dt} = kf(\alpha) \tag{3}$$

$f(\alpha)$ represents the reaction model and k is the rate constant. Using Arrhenius temperature dependence of k, Eq. (3) is written as

$$\frac{d\alpha}{dt} = Aexp\left(-\frac{E}{RT}\right)f(\alpha) \tag{4}$$

By introducing the heating rate (β) and conversion function $f(\alpha) = (1-\alpha)$ Eq. (4) was re-written as;

$$\frac{d\alpha}{dT} = \frac{A}{\beta}exp\left(-\frac{E}{RT}\right)(1-(\alpha)) \tag{5}$$

After mathematical manipulations when α = 0 and T = T_o in Eq. (5), it became;

$$G(\alpha) = \int_0^{\alpha} d\alpha/f(1-\alpha) = ART^2/\beta E\left[1 - 2RT/E\right]exp(-\frac{E}{RT}) \tag{6}$$

After rearranging Eq. (6), and neglecting 2RT/E which is negligible compared with unity, Eq. (6) became;

$$G(\alpha) = (ART^2/\beta E)exp(-E/RT) \tag{7}$$

All data generated through real-time TGA analysis was analyzed by using different isoconversion methods (Flynn–Wall–Ozawa (FWO), Kissenger-Sunose-Akahira (KAS), and Starink) [16–19] to ensure the consistency in experimentation.

Upon rearranging and some mathematical manipulations deviced by ICTAC recommendations, we obtained following equations.

Taking logarithms and rearranging and of both sides of Eq. (7), we obtained Eq. (8)

$$\ln(\frac{\beta}{T^2}) = ln\frac{AE_a}{Rg(\alpha)} - \frac{E_a}{RT} \qquad \text{(KAS)} \tag{8}$$

Integrating Eq. (5) and with the initial conditions,, α = 0, at $T = T_0$, and Doyle's approximation [20] was introduced, and after some mathematical manipulations, we obtained Eq. (9), the final form used by FWO procedure:

$$ln\beta = \ln\frac{AE_a}{Rg(\alpha)} - \frac{E_a}{RT} \qquad \text{(FWO)} \tag{9}$$

Starink method uses the optimized by class of approximations minimizing the deviation between the approximation function and the exact integral.

$$\ln(\frac{\beta}{T^{1.92}}) = ln\frac{AE_a}{Rg(\alpha)} - (1.0008)\frac{E_a}{RT} \qquad \text{(Starink)} \tag{10}$$

Left-hand side of each equation including (8), (9), and (10) were plotted in y-axis against the inverse of combustion temperature in x-axis, and each conversion degree α was applied to calculate kinetic and thermodynamic parameters by compensation effect by the ICTAC kinetics recommendations using following Equations [21].

$$lnA = aE_\alpha + b \tag{11}$$

$$\Delta H = E - RT \tag{12}$$

$$\Delta G = E + RT_m\ln(K_BT_m/hA) \tag{13}$$

The theoretical plots of reaction mechanism were found using following Eq. (14), where θ can be described by ($\theta/\theta_{0.5} = p(x)/p(x_{0.5})$) [21, 22]:

$$\frac{g(\alpha)}{g(0.5)} = \frac{p(x)}{p\left(x_{0.5}\right)} \tag{14}$$

$$x = \frac{E_a}{RT}$$

$$p(x) = \frac{e^{-1.0008x} - 0.312}{x^{1.92}} \tag{15}$$

3 Results and discussion

3.1 Physiochemical analysis

The proximate analysis was conducted on RC samples to determine the moisture, volatile matter and ash contents. The analysis revealed that the moisture content of RC was about 6.6%, which supports the suitability of RC for bioenergy production through combustion. Furthermore, the

promising potential of RC for bioenergy application was further supported by the high volatile matter (80.9%) and low ash (8.82%) contents. Here, the fixed carbon content was calculated using Eq. (1) to be (3.67%). The elemental analyzer was utilized to examine the composition of RC and in particular to identify the carbon, oxygen, nitrogen, sulphur and hydrogen contents, which were reported as 40.52%, 53.22%, 1.41%, 0.1% and 4.95%, respectively. The low traces of hydrogen and sulphur as reported by the ultimate analysis; indicate that RC biomass will not deliver significant amount of toxic gases during the combustion process. The combination of high volatile matter, low ash and toxic components contents illustrate that RC biomass is a valuable candidate for bioenergy production. In fact, volatile matter content of RC biomass is higher than various previously examined and reported biomass samples such as *pine sawdust, Urochloa mutica, rice husk, elephant grass and Miscanthus gigantus* [13, 14, 23, 24]. High heating value (HHV) is another valuable figure to evaluate biomass samples for bioenergy production purposes since HHV demonstrates the amount of energy release during the combustion process. However, HHV requires experimental analysis, which is expensive and subjected to high experimental error [25]. Therefore, different models were proposed to compute HHV and here the following correlation was adopted to compute HHV of RC biomass [25].

$$HHV = 19.288 - 0.2135\frac{VM}{FC} - 1.9584\frac{Ash}{VM} + 0.0234\frac{FC}{Ash} \quad (16)$$

The adopted model was selected since it delivers the least error compare to further models reported in the literature and HHV for RC biomass was computed to be 14.4 MJ kg^{-1}.

3.2 Analyses of TG-DTG curves

The TGA revealed that the increase in reaction temperature resulted in the loss in biomass that was further converted into various other products. During this analysis (TG-DTG curves), thermochemical conversion of the biomass into three states of matter i.e. liquid, solid and gas was represented by the curves during the analysis. These curves showed specific trend, for the understudied samples of the thermal degradation of lignocelluloses when they were put for the comparison to TG-DTG curves (Fig. 1) and it was found for *Cardoon leaves, Red pepper waste, Camel grass, Elephant grass, Rice husk* and *Switchgrass* [26–31].

During thermal degradation, mass loss occurred at a certain temperature and these characteristic temperature ranges. There was a direct proportion between thermal conversion of the sample and heating rate. Thermal conversion of the sample consisted of three stages whereas stage-II had two zones. Temperature in the first stage reached from ambient

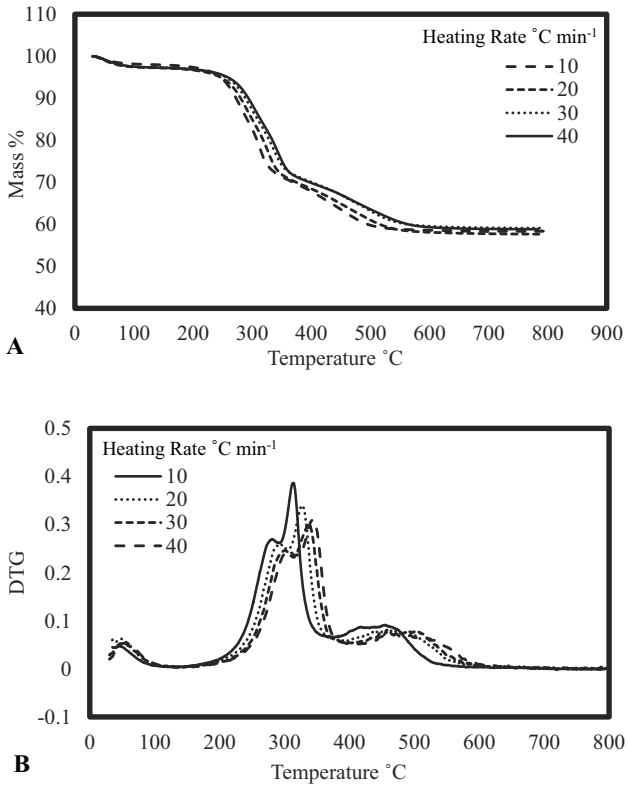

Fig. 1 TG (**A**) and DTG (**B**) curves at four heating rates (10–40 °C min^{-1})

to 210 °C at all heating rates and resulted in the loss of of approximately 11% of mass, which exhibits the evaporation of the moisture content retained within intercellular spaces or compartments. In the second stage, all the heating rates were taken into account and temperature range was 210–370 °C (Region-I) and 370–530 °C (Region-II) that resulted in the maximum of the mass loss i.e. 25% and 14% in both regions respectively. In the third stage temprature was between 530 to 800 ˚C and this stage resulted about 5% of the total mass lost.

Feasible biomass for combustion contains less than 10% of the retained moisture, hence, the sample of the cureent study is a best choice for pyrolysis and combustion [27]. Typical patteren of lignocelluosic biomass was exhibited by thermal transformation. Here, stage-II was responsible for most of the thermal conversion, demonstrating the degradation of pectin, cellulose and hemicellulose where a specific temperature of 210–530 °C was set for their degradation [27]. Temprature ranges in the third stage reflected the degradation of lignin and formation of char [27]. Keeping in view the above trend of these values, it is evident that using *RC* biomass for pyrolysis and combustion possesses represents significant advantage over previously studied biomass samples of *elephant grass, water hyacinth* and *rice husk* [27, 28, 30–32]. Biochar yields of 24.59, 25.45 and 23.67%

were determined at 660 K at three different heating rates, and these yields were comparable to biochar obtained from the combustion and pyrolysis of straw (23.68%) and bran (25.17%) of *rice plant*, and lower than *Para grass* (31.5%) [31], and *Camel grass* (30.46%) [30]. These values suggest for the suitability of the sample for biochar production.

4 Thermokinetics to elucidate the reaction chemistry of RC

Detailed kinetic analyses were performed to calculate different thermodynamic parameters including activation energy (Ea, kJ mol^{-1}), pre-exponential factors (A, s^{-1}), change in enthalpy (ΔH, kJ mol^{-1}) and Gibbs free energy (ΔG, kJ mol^{-1}), and root square of regression (R^2). The combustion reaction mechanism was elucidated through master plots under all heating rates by applying different kinetic models to retain accuracy throughout the modeling process. The reaction mechanism was observed by plotting all the reaction mechanisms of g(α)/g (0.5) and the best plot was compared with experimental data by considering all the reaction models following the ICTAC kinetics recommendations. The perfect match of reaction model was the Fn order (Fig. 2). All regression plots were made by following ICTAC kinetics for all models including KAS, FWO and Starink as shown in Fig. 3. Therefore, all thermodynamic parameters including Ea, A, R^2, ΔH and ΔG were calculated for all α values ranging from 0.1 to 0.9 and are shown in Table 1. The E_a varied between 124 and 218 kJ mol^{-1} with an average value of 161–180 kJ mol^{-1}, furthermore, E_a values remaining decreasing with a minute difference when conversion ranges from 0.1 to 0.6 in all kinetic models. The E_a showed a narrow range (213–143 kJ mol^{-1}) with α ranging from 0.6 to 0.9, where some combustion reaction occurred; it indicates that the combustion was thermodynamically favorable. However, a little increase in E_a was observed after α of 0.7 (Fig. 4). A similar variation trend was observed for ΔH (Fig. 4), where the lower difference between the E_a and ΔH values again demonstrated a thermodynamically favorable reaction. The E_a values of RC during combustion had remarkable resemblance with already studied biomass samples like *pine branch* [33] *pear millet* [13], *Sida cordifolia* L.[12], *beech wood* [34], and *Lentinula edodes* [35]. Therefore, it indicates that the RC reaction chemistry had significant potential into energy-efficient combustion reactions.

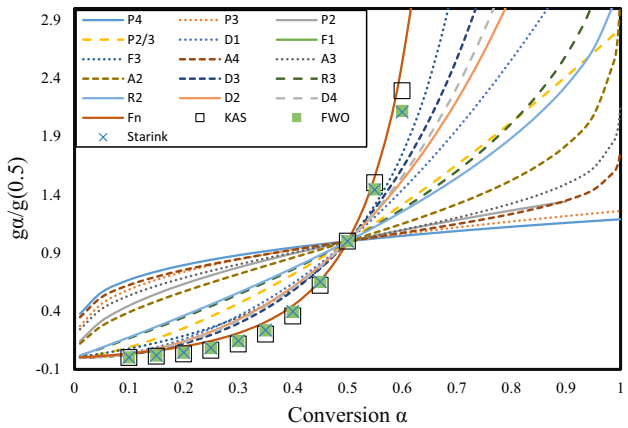

Fig. 2 Reaction mechanism study of Reed Canary

The conversion of biomass to produce products is a complex process due to various reactions involved due to degradation of biomass at different stages as discussed earlier. Many reactions may involve during the combustion of biomass that effect the product formation. The A with several collisions between several compounds elucidates the direct proportion to complexity of biomass. The A showed the nature of the complexity of the reaction. The A of RC may vary from 10^4–10^{13} s^{-1}, the $A < 10^9$ s^{-1} mainly shows the exterior reactions whereas $A \geq 10^9$ s^{-1} shows a simpler complex mechanism [36]. The A values of RC were obtained as 5.90×10^5–1.55×10^{14}, 1.96×10^4–1.39×10^{13}, and 2.24×10^4–1.53×10^{13} as estimated through FWO, KAS and Starink models for α (0.1–0.9), respectively. These values indicated simple reaction kinetics during the chemical conversions. Moreover, the lower energy was required to make activated complex for effective collisions between the molecules. Furthermore, A-values of RC were compared to A-values calculated for *pine branch* [33] *pear millet* [13], *S. cordifolia* L.[12], *beech wood* [34], and *L. edodes* [35] had significant closeness. Moreover, the lower difference between the Ea and ΔH indicated that it would be easy to produce activated complex intermediates by shattering the potential energy barrier [37]. The ΔH values were shown to be ranging from 117 to 207 kJ mol^{-1} for α ranging from 0.2 to 0.9 with an average value of 156–174 kJ mol^{-1} for all the models employed (Table 1). For ΔH, an arc was observed for α 0.1 to 0.6, then there was a rapid rise from 0.7 to 0.9 after a uniform behavior with a minute rise from α: 0.4–0.7 (Fig. 5). Similar differences were observed in some already explored biomass including *tobacco waste* [38], *pine needle* [39], *wheat straw* [40] and *paper mill sludge* [41]. Additionally, ΔG represents the total amount of energy during reaction. The ΔG values explain the array of carbon layers in the biochar produced. Here, ΔG values were ranging from 199 to 253 kJ mol^{-1} at α ranging from 0.1 to 0.9 with an average value of 226–228 kJ mol^{-1} (Fig. 6). The ΔG values showed relevance with the already studied biomass samples in recent studies ranging from 220 to 335 kJ mol^{-1} at various fractional conversions including *tobacco waste* [38], *pine needle* [39], *wheat straw* [40] and *paper mill sludge* [41].

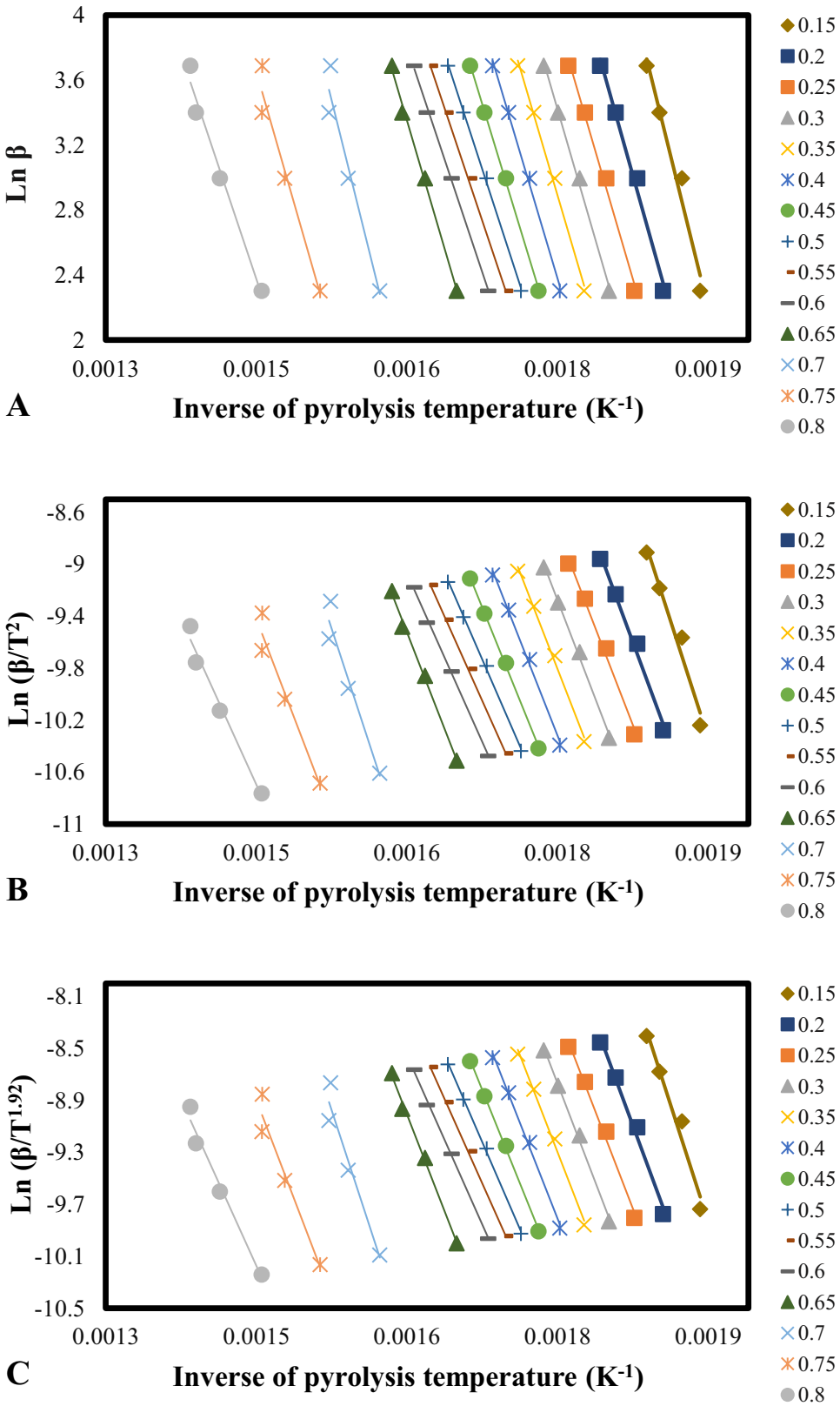

Fig. 3 Best fitting plots of RC (Reed Canary) for (**A**) KAS, (**B**) FWO, (**C**) Starink

Table 1 Thermodynamics parameters of all models

Alpha	E_a kJmol^{-1}	$A\ s^{-1}$	R^2	ΔH kJmol^{-1}	ΔG kJmol^{-1}	E_a kJmol^{-1}	$A\ s^{-1}$	R^2	ΔH kJmol^{-1}	ΔG kJmol^{-1}	E_a kJmol^{-1}	$A\ s^{-1}$	R^2	ΔH kJmol^{-1}	ΔG kJmol^{-1}
FWO						KAS					Starink				
0.1	213.79	4.39E+13	0.990	207.44	207.35	195.12	4.41E+12	0.331	188.77	203.25	195.46	4.83E+12	0.332	189.11	203.01
0.15	218.68	1.55E+14	0.993	212.34	204.24	199.35	1.39E+13	0.968	193.01	200.22	199.71	1.53E+13	0.968	193.36	199.96
0.2	191.64	1.45E+11	0.997	185.29	221.42	173.40	1.23E+10	0.989	167.05	218.83	173.76	1.36E+10	0.989	167.42	218.57
0.25	184.46	2.29E+10	0.996	178.12	225.98	166.41	1.86E+09	0.992	160.06	223.84	166.78	2.06E+09	0.992	160.43	223.57
0.3	185.71	3.15E+10	0.996	179.36	225.18	167.46	2.48E+09	0.996	161.12	223.08	167.84	2.74E+09	0.996	161.50	222.81
0.35	183.66	1.86E+10	0.999	177.32	226.48	165.38	1.41E+09	0.995	159.04	224.58	165.76	1.56E+09	0.995	159.42	224.30
0.4	181.47	1.06E+10	0.999	175.12	227.88	163.16	7.72E+08	0.996	156.81	226.17	163.54	8.57E+08	0.996	157.20	225.89
0.45	177.23	3.54E+09	0.999	170.88	230.57	158.99	2.50E+08	0.999	152.65	229.16	159.38	2.78E+08	0.999	153.04	228.88
0.5	165.84	1.88E+08	0.998	159.50	237.80	148.03	1.29E+07	0.998	141.69	237.01	148.43	1.43E+07	0.998	142.09	236.73
0.55	160.89	5.26E+07	0.997	154.55	240.95	143.22	3.50E+06	0.999	136.88	240.46	143.62	3.90E+06	0.999	137.28	240.18
0.6	161.45	6.07E+07	0.944	155.11	240.59	143.66	3.94E+06	0.998	137.31	240.15	144.06	4.39E+06	0.998	137.71	239.86
0.65	183.74	1.90E+10	0.958	177.39	226.44	164.71	1.17E+09	0.996	158.36	225.06	165.12	1.31E+09	0.996	158.78	224.76
0.7	217.99	1.30E+14	0.981	211.64	204.68	196.86	7.07E+12	0.938	190.52	202.00	197.29	7.94E+12	0.938	190.95	201.69
0.75	187.90	5.55E+10	0.989	181.56	223.79	167.75	2.68E+09	0.953	161.41	222.88	168.20	3.02E+09	0.953	161.85	222.55
0.8	161.04	5.46E+07	0.992	154.70	240.85	141.67	2.30E+06	0.978	135.32	241.58	142.13	2.61E+06	0.978	135.79	241.24
0.85	153.92	8.72E+06	0.954	147.58	245.38	134.45	3.26E+05	0.987	128.10	246.76	134.93	3.71E+05	0.987	128.59	246.41
0.9	143.47	5.90E+05	0.000	137.13	252.01	124.06	1.96E+04	0.991	117.71	254.20	124.56	2.24E+04	0.991	118.22	253.84
Average	180.76			174.41	228.33	161.98			155.64	227.01	162.39			156.04	226.72

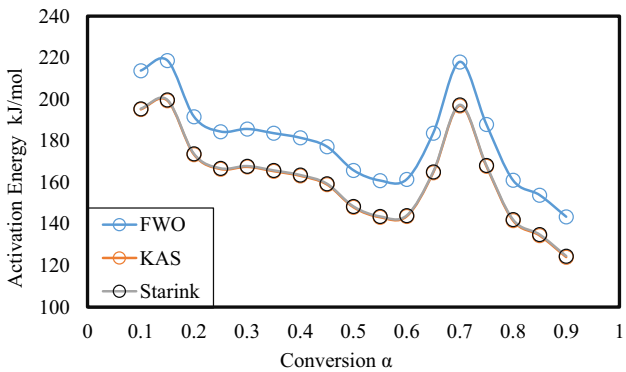

Fig. 4 Comparison between conversion and activation energy values obtained from KAS, FWO and Starink

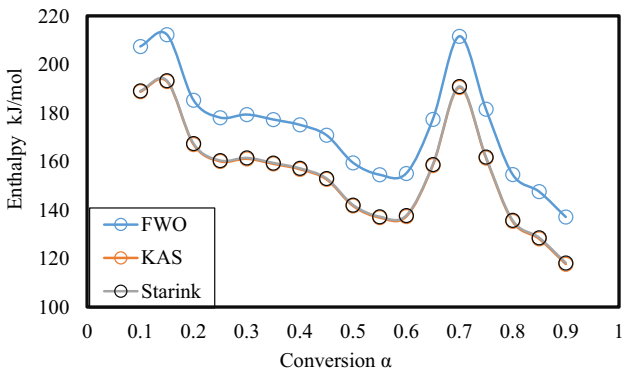

Fig. 5 Comparison between conversion and change in Enthalpy obtained from KAS, FWO and Starink

Taking these values into account, it is concluded that RC has shown to be an easily convertible low-cost source to produce energy and chemicals.

5 Conclusion

The study focused on Reed Canary biomass for bioenergy application due to the free accessibility to the biomass and

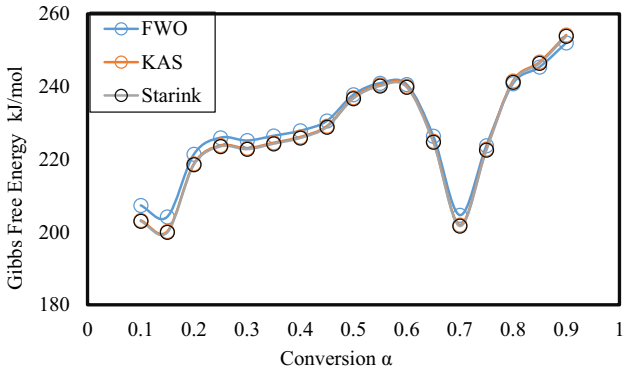

Fig. 6 Comparison between conversion and change in Gibbs free energy obtained from KAS, FWO and Starink

the invasive nature of Reed Canary, which require suitable and environmental friendly approach to control. The combustion behavior of Reed Canary consists of three major thermal degradation zones that can be influenced slightly by the heating rate. These stages are mainly the extraction of the moisture content, followed by the significant mass loss attributed to the decomposition of cellulose, hemicellulose and pectin components. The third stage of thermal degradation represents the formation of char and lignin degradation as depicted by the tail like steady mass loss towards the end of the combustion process. Finally, It was interesting to observed the significant potential of Reed Canary as feedstock for bioenergy production through the thermodynamics properties.

Acknowledgements This project was funded by the Deanship of Scientific Research (DSR) at King Abdulaziz University, Jeddah, under grant no. (RG-5-135-41). The authors, therefore, acknowledge with thanks DSR technical and financial support.

References

1. Smith DJ, Current D, Schulman C, Easter KW (2018) Willingness to produce perennial bioenergy crops: a contingent supply approach. Biomass Bioenerg 117:161–172
2. Sparrevik M, Field JL, Martinsen V, et al (2013) Life cycle assessment to evaluate the environmental impact of biochar implementation in conservation agriculture in Zambia. Environ Sci \& Technol 47:1206–1215
3. Shafiee S, Topal E (2009) When will fossil fuel reserves be diminished? Energy Policy 37:181–189. https://doi.org/10.1016/j.enpol.2008.08.016
4. Al-Hamamre Z, Saidan M, Hararah M et al (2017) Wastes and biomass materials as sustainable-renewable energy resources for Jordan. Renew Sustain Energy Rev 67:295–314
5. Uddin MN, Taweekun J, Techato K et al (2019) Sustainable biomass as an alternative energy source: Bangladesh perspective. Energy Procedia 160:648–654
6. Galanopoulos C, Yan J, Li H, Liu L (2018) Impacts of acidic gas components on combustion of contaminated biomass fuels. Biomass Bioenerg 111:263–277
7. Gumisiriza R, Hawumba JF, Okure M, Hensel O (2017) Biomass waste-to-energy valorisation technologies: a review case for banana processing in Uganda. Biotechnol Biofuels 10:11. https://doi.org/10.1186/s13068-016-0689-5
8. Asadi A, Zhang Y, Mohammadi H et al (2019) Combustion and emission characteristics of biomass derived biofuel, premixed in a diesel engine: a CFD study. Renew Energy 138:79–89
9. White JE, Catallo WJ, Legendre BL (2011) Biomass pyrolysis kinetics: a comparative critical review with relevant agricultural residue case studies. J Anal Appl Pyrolysis 91:1–33. https://doi.org/10.1016/j.jaap.2011.01.004
10. Liu G, Liao Y, Guo S et al (2016) Thermal behavior and kinetics of municipal solid waste during pyrolysis and combustion process. Appl Therm Eng 98:400–408
11. Kalogirou SA (2003) Artificial intelligence for the modeling and control of combustion processes: a review. Prog Energy Combust Sci 29:515–566. https://doi.org/10.1016/S0360-1285(03)00058-3
12. Boubacar Laougé Z, Merdun H (2020) Pyrolysis and combustion kinetics of Sida cordifolia L. using thermogravimetric analysis. Bioresour Technol 299:122602. https://doi.org/10.1016/j.biortech.2019.122602
13. Boubacar Laougé Z, Merdun H (2020) Kinetic analysis of Pearl Millet (Penissetum glaucum (L.) R. Br.) under pyrolysis and combustion to investigate its bioenergy potential. Fuel 267:117172. https://doi.org/10.1016/j.fuel.2020.117172
14. Xu X, Pan R, Chen R (2021) Combustion characteristics, kinetics, and thermodynamics of pine wood through thermogravimetric analysis. Appl Biochem Biotechnol 1–20
15. Gupta S, Gupta GK, Mondal MK (2020) Thermal degradation characteristics, kinetics, thermodynamic, and reaction mechanism analysis of pistachio shell pyrolysis for its bioenergy potential. Biomass Convers Biorefinery 1–15
16. Akahira T, Sunose T (1969) Transactions of Joint Convention of Four Electrical Institutes. 246
17. Ozawa T (1965) A new method of analyzing thermogravimetric data. Bull Chem Soc Jpn 38:1881–1886
18. Flynn JH, Wall LA (1966) A quick, direct method for the determination of activation energy from thermogravimetric data. J Polym Sci Part B Polym Lett 4:323–328
19. Starink MJ (2003) The determination of activation energy from linear heating rate experiments: a comparison of the accuracy of isoconversion methods. Thermochim Acta 404:163–176
20. Doyle CD (1961) Kinetic analysis of thermogravimetric data. J Appl Polym Sci 5:285–292
21. Vyazovkin S, Chrissafis K, Di Lorenzo ML et al (2014) ICTAC Kinetics Committee recommendations for collecting experimental thermal analysis data for kinetic computations. Thermochim Acta 590:1–23. https://doi.org/10.1016/j.tca.2014.05.036
22. Gotor FJ, Criado JM, Malek J, Koga N (2000) Kinetic analysis of solid-state reactions: the universality of master plots for analyzing isothermal and nonisothermal experiments. J Phys Chem A 104:10777–10782. https://doi.org/10.1021/jp0022205
23. Machado JC, Carneiro PCS, da Costa CJ et al (2017) Elephant grass ecotypes for bioenergy production via direct combustion of biomass. Ind Crops Prod 95:27–32
24. Paniagua S, Prado-Guerra A, García AI, Calvo LF (2019) Bioenergy derived from an organically fertilized poplar plot: overall TGA and index estimation study for combustion, gasification, and pyrolysis processes. Biomass Convers Biorefinery 9:749–760. https://doi.org/10.1007/s13399-019-00392-7
25. Nhuchhen DR, Salam PA (2012) Estimation of higher heating value of biomass from proximate analysis: a new approach. Fuel 99:55–63

26. Xu Y, Chen B (2013) Investigation of thermodynamic parameters in the pyrolysis conversion of biomass and manure to biochars using thermogravimetric analysis. Bioresour Technol 146:485–493
27. Braga RM, Melo DMA, Aquino FM et al (2014) Characterization and comparative study of pyrolysis kinetics of the rice husk and the elephant grass. J Therm Anal Calorim 115:1915–1920
28. Biney PO, Gyamerah M, Shen J, Menezes B (2015) Kinetics of the pyrolysis of arundo, sawdust, corn stover and switch grass biomass by thermogravimetric analysis using a multi-stage model. Bioresour Technol 179:113–122
29. Maia AAD, de Morais LC (2016) Kinetic parameters of red pepper waste as biomass to solid biofuel. Bioresour Technol 204:157–163
30. Mehmood MA, Ye G, Luo H et al (2017) Pyrolysis and kinetic analyses of Camel grass (Cymbopogon schoenanthus) for bioenergy. Bioresour Technol 228:18–24
31. Ahmad MS, Mehmood MA, Al Ayed OS et al (2017) Kinetic analyses and pyrolytic behavior of Para grass (Urochloa mutica) for its bioenergy potential. Bioresour Technol 224:708–713
32. Huang L, Liu J, He Y et al (2016) Thermodynamics and kinetics parameters of co-combustion between sewage sludge and water hyacinth in CO 2/O 2 atmosphere as biomass to solid biofuel. Bioresour Technol 218:631–642
33. Niu H, Liu N (2015) Thermal decomposition of pine branch: unified kinetic model on pyrolytic reactions in pyrolysis and combustion. Fuel 160:339–345
34. Ding Y, Huang B, Wu C et al (2019) Kinetic model and parameters study of lignocellulosic biomass oxidative pyrolysis. Energy 181:11–17
35. Zou H, Evrendilek F, Liu J, Buyukada M (2019) Combustion behaviors of pileus and stipe parts of Lentinus edodes using thermogravimetric-mass spectrometry and Fourier transform infrared spectroscopy analyses: thermal conversion, kinetic, thermodynamic, gas emission and optimization analyses. Bioresour Technol 288:121481
36. Turmanova SC, Genieva SD, Dimitrova AS, Vlaev LT (2008) Non-isothermal degradation kinetics of filled with rise husk ash polypropene composites. Express Polym Lett 2:133–146
37. Ahmad MS, Mehmood MA, Ye G et al (2017) Thermogravimetric analyses revealed the bioenergy potential of Eulaliopsis binata. J Therm Anal Calorim. https://doi.org/10.1007/s10973-017-6398-x
38. Wu W, Mei Y, Zhang L et al (2015) Kinetics and reaction chemistry of pyrolysis and combustion of tobacco waste. Fuel 156:71–80
39. Chen R, Li Q, Xu X, et al (2020) Combustion characteristics, kinetics and thermodynamics of Pinus Sylvestris pine needle via non-isothermal thermogravimetry coupled with model-free and model-fitting methods. Case Stud Therm Eng 22:100756
40. Rathore NS, Pawar A, Panwar NL (2021) Kinetic analysis and thermal degradation study on wheat straw and its biochar from vacuum pyrolysis under non-isothermal condition. Biomass Convers Biorefinery 1–13
41. Yaras A, Demirel B, Akkurt F, Arslanoglu H (2021) Thermal conversion behavior of paper mill sludge: characterization, kinetic, and thermodynamic analyses. Biomass Convers Biorefinery. https://doi.org/10.1007/s13399-020-01232-9